



Modeling study of PM_{2.5} pollutant transport across cities in China's Jing–Jin–Ji region during a severe haze episode in December 2013

C. Jiang¹, H. Wang², T. Zhao¹, T. Li¹, and H. Che²

¹Nanjing University of Information Science & Technology, Nanjing 210044, China

²Institute of Atmospheric Composition, Chinese Academy of Meteorological Sciences (CAMS), CMA, Beijing, 100081, China

Correspondence to: C. Jiang (jc452@163.com) and H. Wang (wangh@cams.cma.gov.cn)

Received: 31 October 2014 – Published in Atmos. Chem. Phys. Discuss.: 10 February 2015

Revised: 7 May 2015 – Accepted: 7 May 2015 – Published: 26 May 2015

Abstract. To study the influence of particulate matter (PM) transported from surrounding regions on the high PM_{2.5} pollution levels in Beijing, the GRAPES-CUACE model was used to simulate a serious haze episode that occurred on 6–7 December 2013. The results demonstrate the model's suitability for describing haze episodes throughout China, especially in the Beijing–Tianjin–Hebei (Jing–Jin–Ji) region. A very close positive correlation was found between the southerly wind speed over the plain to the south of Beijing and changes in PM_{2.5} in Beijing, both reaching maximum values at about 900 hPa, suggesting that the lower atmosphere was the principal layer for pollutant PM transport from its southern neighbouring region to Beijing. During haze episodes, and dependent upon the period, Beijing was either a pollution source or sink for its surrounding area. PM input from Beijing's environs was much higher than the output from the city, resulting in the most serious pollution episode, with the highest PM_{2.5} values occurring from 00:00 to 10:00 UTC (08:00 to 18:00 LT), 7 December 2013. PM pollutants from the environs of the city accounted for over 50 % of the maximum PM_{2.5} values reached in Beijing. At other times, the Beijing area was a net contributor to pollution in its environs.

ment, human health and ecosystems (Kan et al., 2012; Liu et al., 2012). China's air pollution has become increasingly serious since the economic reforms of 1978, which allowed rapid economic development. Gross domestic product has grown by about 10 % per annum (China Statistical Yearbook 2012, 2013). China is now considered to be one of the engines of global economic growth, but this rapid growth has resulted in an increase in energy consumption, air pollution, and associated health effects (Chan and Yao, 2008).

In recent years, haze has become a major pollution problem in Chinese cities (Wu et al., 2010; Du et al., 2011; Tan et al., 2011). Under the observation standards released by the China Meteorological Administration (CMA), haze is defined as a pollution phenomenon characterized by deteriorated horizontal visibility of < 10 km, caused by fine particulate matter (PM) suspended in the atmosphere (CMA, 2003). Haze occurs when sunlight is absorbed and scattered by high concentrations of atmospheric aerosols (E. Kang et al., 2013; Salinas et al., 2013). It has a negative impact on human health and the environment (Wu et al., 2005; Gurjar et al., 2010), and it also has a climate change effect over a regional or global scale by altering solar and infrared radiation in the atmosphere (Wang et al., 2011; Yu et al., 2011; Chen et al., 2012).

With an increasing number of local and regional haze events reported by the media, much attention has been paid to reducing air pollutant emissions and to improving air quality across the cities (Huang et al., 2013; H. Kang et al., 2013; Xu et al., 2013; Tan et al., 2015), municipalities and provinces of China (Cheng et al., 2014; Ji et al., 2014). The Jing–Jin–Ji region, located in central–eastern China, is not only one of

1 Introduction

Air pollution has become a serious problem in megacities around the world (Kanakidou et al., 2011), and the topic has been receiving increased attention because of the close relationship between air pollution and the atmospheric environ-

China's most economically developed and industrialized regions, but is the area that most frequently experiences haze episodes (Ji et al., 2014; Wang et al., 2014a; L. T. Wang et al., 2014). Beijing, at the center of the Jing–Jin–Ji region, is one of China's most economically developed cities, and has suffered from increasingly severe haze events (Duan et al., 2012; Wang et al., 2012; Liu et al., 2014; Quan et al., 2014). It is vital that air pollution in Beijing is studied in detail so as to inform policy aimed at averting irreversible environmental damage (Cheng et al., 2013; Zhang et al., 2014). The other areas of the Jing–Jin–Ji region should also be studied, as they are important components of the wider region and affect Beijing directly via the transport of PM pollutants (Fu et al., 2014; Ying et al., 2014). In the present reported study, an online mesoscale haze forecasting model was used to study the transport of major air pollutants to and from Beijing and the other areas of the Jing–Jin–Ji region (Wang et al., 2013).

2 Modeling

2.1 Model description

The new-generation Global/Regional Assimilation and Prediction System (GRAPES_Meso) and the Chinese Unified Atmospheric Chemistry Environment (CUACE) model developed by the Chinese Academy of Meteorological Science (CAMS), the CMA, were integrated to build an online chemical weather forecasting model, GRAPES-CUACE, focusing especially on haze pollution forecasting in China and East Asia (Zhang and Shen, 2008; Wang et al., 2009). GRAPES_Meso was adopted as the numerical weather prediction model for aerosol determination. It is a new-generation general hydrostatic/non-hydrostatic, multi-scale numerical model developed by the Research Center for Numerical Meteorological Prediction, CAMS, CMA (Zhang and Shen, 2008). The model uses standardized and module-based software and has been developed in accordance with strict software engineering requirements, including program-operated parallel calculations (Xue et al., 2008). Testing has shown that the design and application of the model meet these prerequisites, and that it can therefore serve as a good foundation for the sustainable development of a numerical prediction system for China (Chen et al., 2008). The large-scale horizontal and vertical transportation and diffusion processes for all gases and aerosols can also be processed using GRAPES_Meso's dynamic framework (Xu et al., 2008). Again, testing has demonstrated that both the design of the model's framework and its implementation meet the requirements of real-time operational weather forecasting, especially in China and East Asia. GRAPES_Meso has therefore been used as an operational, real-time, short-term weather prediction system in China since 2009 (Yang et al., 2008; Zhu et al., 2008).

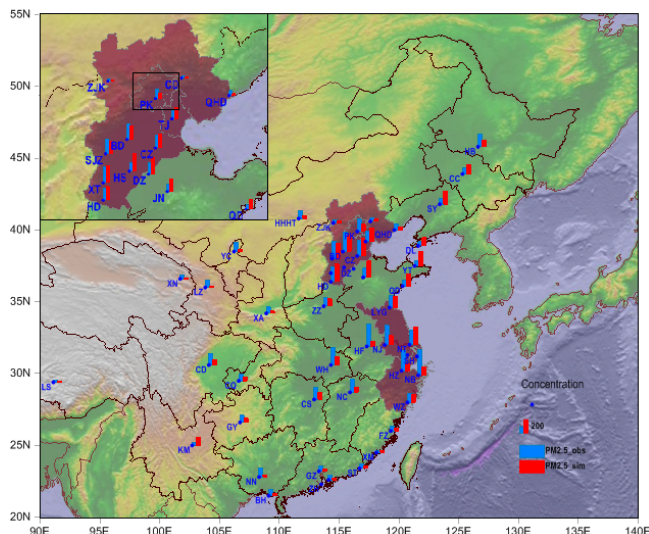


Figure 1. Mean observed and simulated PM_{2.5} ($\mu\text{g m}^{-3}$) for 6–7 December 2013.

The CUACE model was developed by the CAMS Centre for Atmosphere Watch And Services (CAWAS). It is a newly developed system for testing and forecasting air quality in China that includes four functions: treating aerosols; gas-phase chemistry; emissions; and data assimilation (Gong and Zhang, 2008). The detailed data capture by this model of processes such as aerosol sources, transport, dry and wet deposition, and dust removal both in and below clouds, clearly describes the interaction between aerosols and clouds (Zhou et al., 2008). CUACE has been designed as a unified chemistry module that can be easily coupled with any atmospheric model (e.g. regional air quality and climate models) on various temporal and spatial scales. It has thus been integrated online with GRAPES_Meso to produce the GRAPES-CUACE model (Wang et al., 2009, 2010, 2015a). Dust particles are divided into 12 size bins (Gong et al., 2003), following guidelines provided by the measurement of soil dust size in Chinese desert regions during 1994–2001 (Zhang et al., 2003).

2.2 Model domain and parameters

In this study, GRAPES-CUACE was used to simulate a haze episode in December 2013. The model's vertical cap was set at about 30 km, with 31 vertical layers. As shown in Fig. 1, its domain covered the East Asia region (20–55° N, 90–140° E) with a horizontal resolution of $0.25^\circ \times 0.25^\circ$. National Centers for Environmental Prediction (NCEP) $1^\circ \times 1^\circ$ reanalysis data were used for the model's initial and 6 h meteorological lateral direction input fields. The model ran at 00:00 UTC every day, based on NCEP reanalysis data and the chemical tracer initial field, and the simulation time is 48 h. The monthly mean values of all tracers from observation data are used for initialization at the very beginning of the model run.

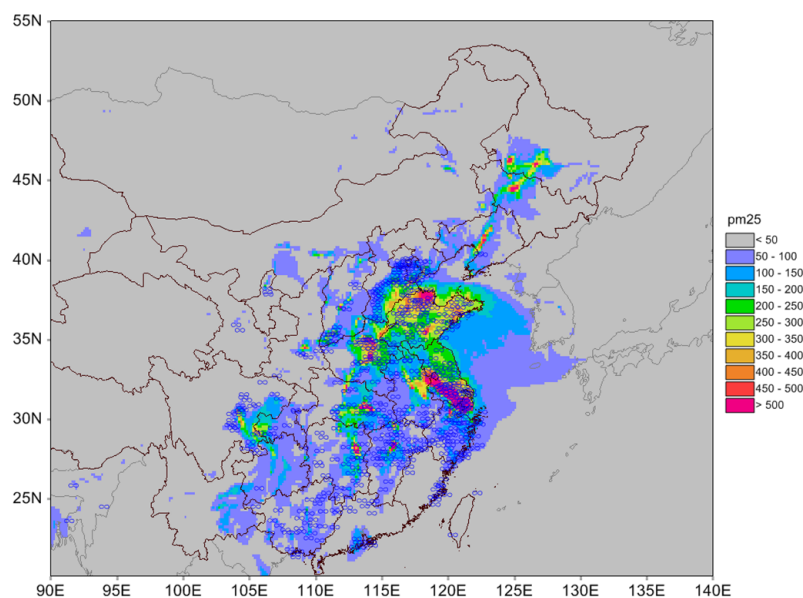


Figure 2. Simulated PM_{2.5} (shaded) and haze weather phenomena observed at 14:00 UTC (22:00 LT), 7 December 2013.

The initial values of all gases in RADM2 and aerosol concentrations are based on the 24 h forecast made by the previous day's model run. The simulation results from 00 to 24 h are used in this study. The model simulation begins from 26 November and the results of 1–31 December are used in order to avoid the uncertainties from the initial chemical fields at the model start.

3 Data description

This study employed CMA ground visibility and operational weather observation data. The data covered mainland China, including a total of 600 ground observation stations.

The daily mean PM_{2.5} concentrations were from surface observations made by the China National Environmental Monitoring Center (CNEMC, <http://www.cnpm25.com>). They included values for 74 cities in mainland China. The data represented the mean values of data from different observation stations distributed in various downtown, suburb, and suburban areas of each city. For example, pollutant concentrations in Beijing were obtained by extracting the mean value from the data from 12 observation sites. This value was then used to represent the mean pollution conditions for each city as a whole.

Detailed high-resolution emission inventories of reactive gases from emissions over China in 2007, i.e. for SO₂, NO_x, CO, NH₃, and volatile organic compounds (VOCs), were updated to form current emission data, based on official national emission source criteria (Cao et al., 2006, 2010). The Sparse Matrix Operator Kernel Emissions (SMOKE) system was used to transform these emission data into the hourly gridded data required by the GRAPES_CUACE model, in-

cluding the five aerosol species of black carbon (BC), organic carbon (OC), sulfate, nitrate, and fugitive dust particles, in addition to 27 gases, such as VOCs, NH₃, CO, CO₂, SO_x and NO_x (An et al., 2013). Modified SMOKE was used according to GRAPES_CUACE, which is similar to the RADM II chemical mechanism. The detailed introduction of chemical species and chemical mechanisms was given in several papers (Gong and Zhang, 2008; Wang et al., 2015b).

4 Results

4.1 Model evaluation

First, the simulation results were compared with the observation data from the major cities in the Jing–Jin–Ji region during the haze episode of 6–7 December to evaluate the model's capabilities. The Jing–Jin–Ji region and the Yangtze River delta (YRD) region were the most severely polluted during 6–7 December, with mean observed PM_{2.5} values for the 2-day period of about 200 µg m⁻³ (Fig. 1). The simulated PM_{2.5} concentrations are in good agreement with observations for most of the cities, especially in the Jing–Jin–Ji region (e.g. Baoding (BD), Beijing (BJ), Cangzhou (CZ), Chengde (CD), Dezhou (DZ), Jinan (JN), Handan (HD), Hengshui (HS), Qinhuangdao (QHD), Shijiazhuang (SJZ), Tianjin (TJ), Xingtai (XT) and Zhangjiakou (ZJK)). Both data sets showed that cities in the northern Jing–Jin–Ji region experienced lower levels of pollution and were less affected by PM_{2.5} during this haze episode (e.g. ZJK, CD, and QHD, with observed PM_{2.5} concentrations of 59.1, 51.9 and 94.1 µg m⁻³, respectively, and simulated PM_{2.5} concentrations of 30.9, 44.3 and 60.1 µg m⁻³, respectively), while the

cities in the central and southern sectors of the Jing–Jin–Ji region experienced severe pollution and high PM_{2.5} levels (e.g. BJ, TJ, BD, CZ, SJZ, HS, XT, HD, DZ and JN, with observed PM_{2.5} concentrations of 194.3, 165.6, 302.1, 237.3, 268.7, 160.1, 295.1, 223.3, 224.3 and 149.9 $\mu\text{g m}^{-3}$, respectively, and simulated PM_{2.5} concentrations of 115.7, 207.1, 250.1, 267.0, 237.7, 326.5, 323.3, 263.6, 312.1 and 256.1 $\mu\text{g m}^{-3}$, respectively). The modeled results thus accurately described the haze episode over the whole region.

The horizontal distribution of simulated PM_{2.5} concentrations was compared with observed haze weather phenomena in eastern China. The centralized hazy weather observed in the region at 14:00 UTC (22:00 LT), 7 December 2013, corresponded to the area of high simulated PM_{2.5} (Fig. 2). Simulated PM_{2.5} values were $> 150 \mu\text{g m}^{-3}$ for the whole of eastern China, with most areas of the highest concentration reaching $300 \mu\text{g m}^{-3}$ or even $500 \mu\text{g m}^{-3}$. Hazy weather was concentrated in the Jing–Jin–Ji region, i.e. Shandong, Jiangsu, and Zhejiang provinces, and Shanghai. There were clearly delineated areas of high simulated PM_{2.5} values that corresponded to these regions.

There was an obvious demarcation line with respect to observed visibility from the southwest to the northeast, dividing China into high visibility and low visibility regions, with the low visibility region centered on the YRD (Fig. 3). The simulated visibility showed similar results (Fig. 3), albeit it was lower than the observed visibility in Shandong, southern Hebei and Shanxi provinces.

Several major cities, including BJ, BD, CZ, DZ, HD, HS, SJZ, XT and Zhengzhou (ZZ) in the Jing–Jin–Ji region and its environs, and Shanghai (SH) and Nanjing (NJ) in the YRD, were selected for a comparison of daily average observed and simulated PM_{2.5} values during 1–31 December 2013, to test the validity of long-term simulations. As shown in Fig. 4, the simulated daily results were fairly close to the observed values for the 6–7 December haze episode. Beginning on 6 December, this episode was most severe on 7 December; and then PM_{2.5} levels decreased rapidly from 8 December onwards. The simulated results for Beijing and the average of whole Jing–Jin–Ji region were highly consistent with the trends in observed daily values for the whole of December. Simulated results for the other cities in the Jing–Jin–Ji region also showed close correlation with observed data for 6–7 December, even considering that the maximum value appeared 1 day earlier in HS and 1 day later in SH. While the simulated values for NJ were lower than the observed data, they essentially exhibited the same daily trends.

The results obtained by GRAPES-CUACE for the Jing–Jin–Ji region through its simulation of PM_{2.5} concentrations demonstrate the model's suitability for studying the impact of particulate transport on PM_{2.5} concentrations. The Jing–Jin–Ji region was therefore chosen as an appropriate study area.

4.2 Wind field

Beijing is currently experiencing the severest haze pollution in its history. On the plains of Hebei to the south, the most seriously polluted area in China, haze and fog episodes are much more serious even than in Beijing. Seven of the 10 cities with the highest levels of PM_{2.5} pollution in China are located in this region (Wang et al., 2014a, 2014b). The contribution made by cross-city pollutants transported from southern Hebei Province to levels of PM_{2.5} pollution in BJ is receiving much attention. The construction of the wind field over this region, particularly the wind field pattern in the planetary boundary layer (PBL), is a key factor in determining the impact of the cross-city transport of PM_{2.5} pollutants.

The wind field was analysed to study the impact that PM transport from its environs had on air pollution in BJ during the haze episode of the present study. As Fig. 5a shows, PM_{2.5} concentrations in BJ reached their maximum at 08:00 UTC (16:00 LT), 7 December. Stable southwesterly winds affected BJ and the area to the south of BJ, while the wind direction was northwesterly and the wind speed lower in the region to the north of BJ. From both the observed and simulated data (Figs. 1, 2, and 3), it is apparent that the region to the south of BJ was the most polluted area, with the highest PM_{2.5}, lowest visibility and densest haze, and this region was therefore the likely main contributor to pollution levels in BJ during this haze episode. The vertical section along 115.25° E (Fig. 5b) enabled us to explore the relationship between the wind field and PM_{2.5} concentrations and transport at different vertical heights. Figure 5b shows a southwesterly wind at 39° N blowing from the surface to the 800 hPa level in the region's southern sector. In the southern sector closest to BJ, the southerly wind speed reached its maximum value at about 900 hPa; and PM_{2.5} also exhibited high values at the same height. Pollutants could thus be transported to BJ by the stable southwesterly wind from the southern environs via the 900 hPa layer. The northerly, or very weak southerly, wind in the region north of 41° N , together with the southerly wind south of 39° N , led to the formation of a wind convergence field over BJ stretching from the surface level to 900 hPa. This would have been beneficial to the accumulation of PM_{2.5} and the consequent aggravation of haze. The vertical section along 39.375° N describes a southerly wind in the region to the south of BJ from 116 to 125° E (Fig. 5c). This southerly wind, extending from the surface to 800 hPa, reached its maximum velocity at 900 hPa in the area to the south of BJ (116 to 118° E). PM_{2.5} concentrations were also significantly higher in this region; pollutants from the 116 – 125° E area would have been easily transported northward by the southerly wind. BJ was most likely affected by this process, raising pollution levels and aggravating the haze.

To verify these results, we analysed the relationship between PM_{2.5} concentrations in BJ and the wind field of the area to the south of BJ (i.e. 113.5 – 118° E , 34.5 – 39.5° N) (Fig. 5a). In the analysis, positive average hourly wind speed

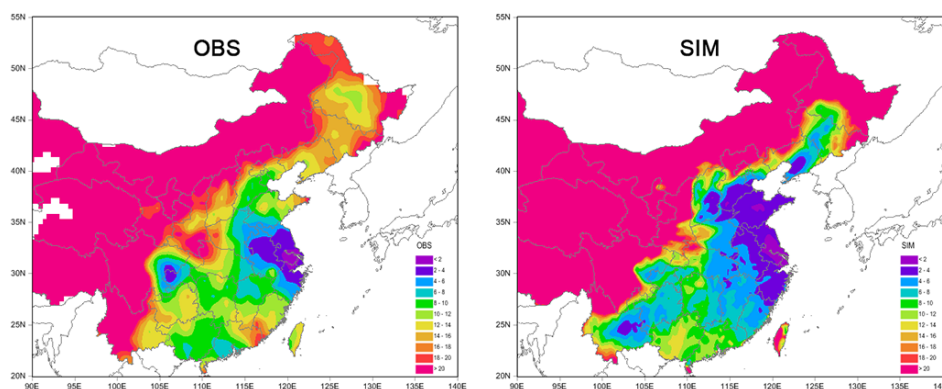


Figure 3. Mean (a) observed and (b) simulated visibility for 6–7 December 2013.

(v) values were representative of a southerly wind, and negative v values a northerly wind. The results showed that, when there was southerly wind in the area to the south of BJ, average PM_{2.5} concentrations in BJ always increased (Fig. 6). This was most obvious on 7 December, when the highest PM_{2.5} values occurred, accompanied by longer periods of stable southerly winds. When there was a northerly wind in the area to the south of BJ, average PM_{2.5} concentrations in BJ fell, and then stabilized.

4.3 BJ's PM_{2.5} input and output

To investigate the contribution of PM_{2.5} transported from its surroundings to BJ pollution levels, the transport rates (kg s⁻¹) for PM_{2.5} from four directions, east (E), west (W), south (S) and north (N), were calculated using the following formulas:

$$\begin{aligned} \text{Tran}_N(t) &= \sum_{z=1}^7 \sum_{x=x_1}^{x_2} \text{PM}_{y_1}(x, z, t) \cdot \Delta x_{y_1} \cdot \Delta z_{y_1}(x, z) \\ &\quad \cdot v_{y_1}(x, z, t) \\ \text{Tran}_S(t) &= - \sum_{z=1}^7 \sum_{x=x_1}^{x_2} \text{PM}_{y_2}(x, z, t) \cdot \Delta x_{y_2} \cdot \Delta z_{y_2}(x, z) \\ &\quad \cdot v_{y_2}(x, z, t) \\ \text{Tran}_E(t) &= \sum_{z=1}^7 \sum_{y=y_1}^{y_2} \text{PM}_{x_1}(y, z, t) \cdot \Delta y(y) \cdot \Delta z_{x_1}(y, z) \\ &\quad \cdot u_{x_1}(y, z, t) \\ \text{Tran}_W(t) &= - \sum_{z=1}^7 \sum_{y=y_1}^{y_2} \text{PM}_{x_2}(y, z, t) \cdot \Delta y(y) \cdot \Delta z_{x_2}(y, z) \\ &\quad \cdot u_{x_2}(y, z, t) \\ \text{Tran}_{\text{net}}(t) &= \text{Tran}_N(t) + \text{Tran}_S(t) + \text{Tran}_W(t) + \text{Tran}_E(t), \end{aligned}$$

where Tran_N , Tran_S , Tran_E and Tran_W represent the PM_{2.5} transport rate for N, S, E and W, respectively (Fig. 7). Positive Tran values indicated net pollutant input into BJ; negative Tran values described net pollutant output from BJ. PM

stands for PM_{2.5} concentration; x_1 , x_2 (Fig. 7) are the westernmost and easternmost BJ longitudes, respectively, and the subscripts y_1 , y_2 (Fig. 7) are the southernmost and northernmost BJ latitudes; t stands for time; Δx , Δy , Δz indicate the individual grid distances of the x , y , and z axes; u stands for the easterly/westerly wind speed (negative for easterly wind); and v stands for the southerly/northerly wind speed (negative for northerly wind). The constantly negative PM_{2.5} transport rate toward BJ, reaching a maximum rate of -112.8 kg s^{-1} at 11:00 UTC (19:00 LT) in the southerly direction, indicated a constant output of PM_{2.5} southward from BJ to its southern environs on 6 December (Fig. 8a). Eastward PM_{2.5} transport rates were largely negative before 12:00 UTC (20:00 LT), indicating net PM_{2.5} output from BJ downwind. After 12:00 UTC (20:00 LT), the PM_{2.5} transport rate became slightly positive and then remained steady, indicating a small net input in the afternoon. There was little westerly or northerly transport throughout the day.

The total input/output rate was calculated by summing the input/output transport rate for the four directions; and the net transport rate was obtained by summing the total input and output rate. Positive net transport values indicated that the BJ area was receiving PM_{2.5} from its surroundings; negative net values showed BJ to be exporting PM_{2.5} to its surroundings. The total output rate clearly exceeded the input rate, and the net transport rate was negative, indicating a net output of pollutants from BJ during the period 00:00–13:00 UTC (08:00–21:00 LT), 6 December (Fig. 8b). After 14:00 UTC (22:00 LT), the output rate clearly fell, while the input rate remained substantially unchanged, resulting in the net transport rate falling close to 0. This shows that the BJ area was a source of pollutants for the areas to its east and south throughout the whole of 6 December.

For 7 December (the most polluted day in this episode), transport rate values for each direction changed substantially (Fig. 8c). There were large positive values for westerly and southerly winds, indicating major PM_{2.5} transport from these directions to BJ; and this correlates with the inferences drawn from Figs. 5 and 6. The transport rate eastward was always

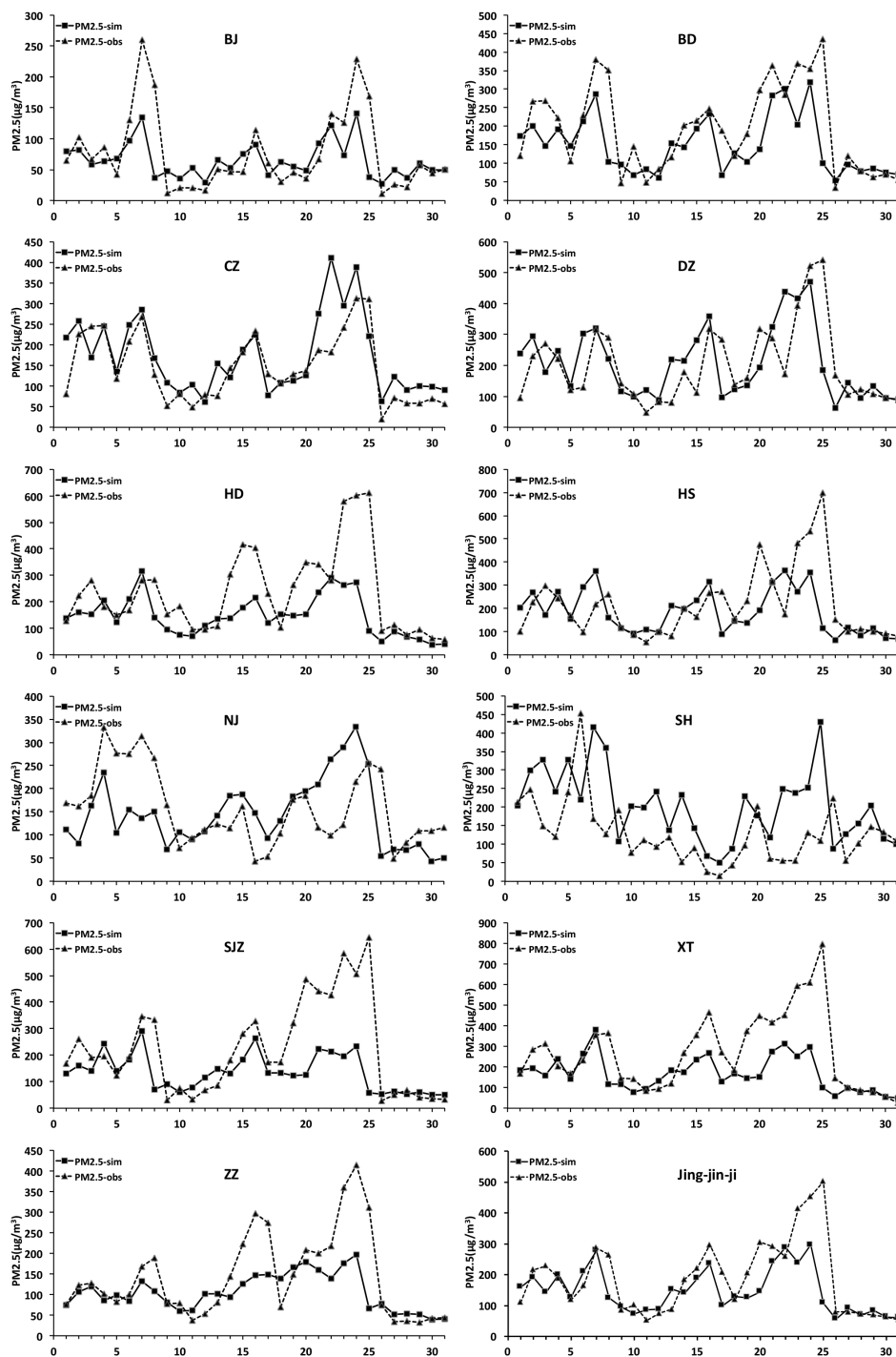


Figure 4. Daily variations in observed and simulated PM_{2.5} ($\mu\text{g m}^{-3}$) for 1–31 December 2013 at stations in BJ, BD, CZ, DZ, HD, HS, NJ, SH, SJZ, XT, ZZ and the whole Jing–Jin–Ji.

positive, reaching a maximum of 149.5 kg s^{-1} at 08:00 UTC (16:00 LT); it was always negative in the westward direction, reaching a minimum of -174.2 kg s^{-1} at 12:00 UTC (20:00 LT). This suggests that a westerly wind dominated on 7 December and transported PM_{2.5} from the area to the

west of BJ to the city and to its eastern downwind area. PM_{2.5} transport was heaviest at 08:00 UTC (16:00 LT) and 12:00 UTC (20:00 LT) from the west and east, respectively. There was input from the south and output northward before 11:00 UTC (19:00 LT), with concurrent maxima of 86.4

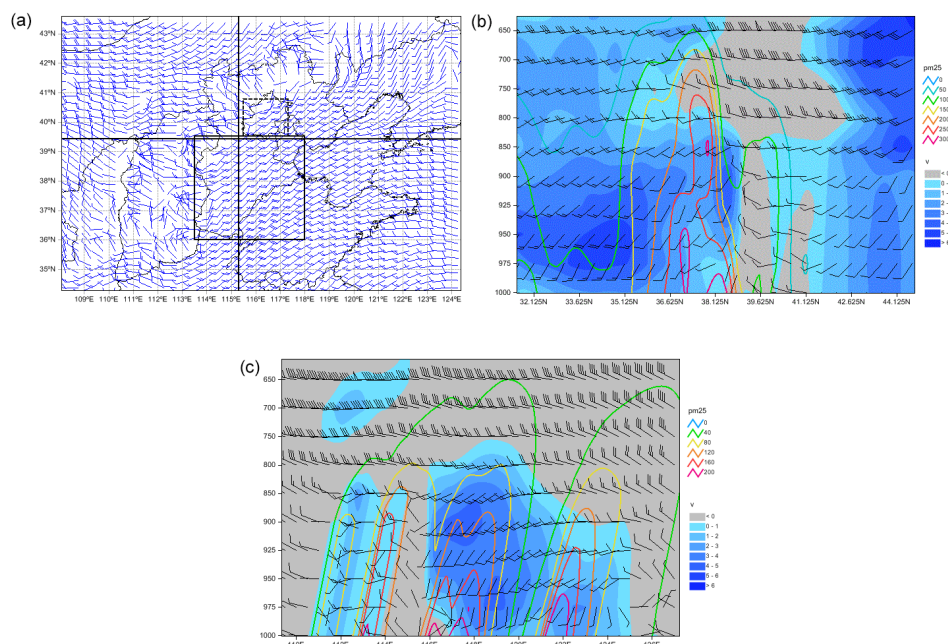


Figure 5. (a) Horizontal wind field at 900 hPa, and its vertical section at (b) 115.25° E and (c) 39.375° N at 08:00 UTC (16:00 LT), 7 December 2013.

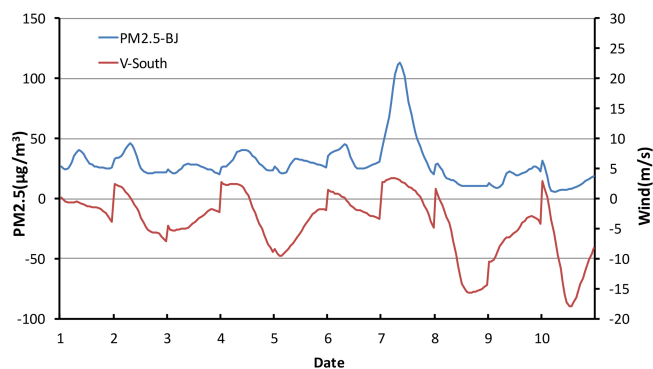


Figure 6. Hourly variations in PM_{2.5} ($\mu\text{g m}^{-3}$) in BJ and mean southerly wind speed (negative for northerly wind) for the region to the south of BJ, 1–10 December 2013.

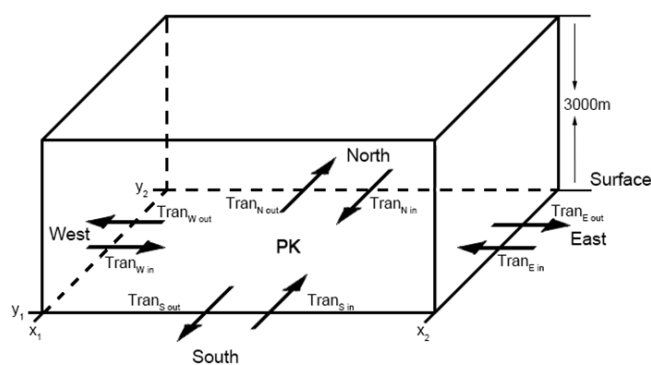


Figure 7. Schematic diagram of pollutant transport between BJ and its surrounding regions.

and 22.6 kg s^{-1} at 08:00 UTC (16:00 LT), respectively. After 12:00 UTC (20:00 LT), the wind direction became northerly, leading to a reversal in the direction of input/output pollutant transport. Net pollutant output turned southward; the output rate was clearly greater than the input rate from the north during the period 12:00–24:00 UTC, 7 December (20:00 LT, 7 December to 08:00 LT, 8 December).

The net transport rate for BJ on 7 December was positive before 10:00 UTC (18:00 LT), rising from about 0 to a maximum of 118.1 kg s^{-1} at 06:00 UTC (14:00 LT), and then began to decline to consistently negative values after 11:00 UTC (19:00 LT) (Fig. 8d). This suggests that the input of pollutants into BJ exceeded the output during the pe-

riod 00:00–10:00 UTC (08:00–18:00 LT). After 11:00 UTC (19:00 LT), input transport rates into BJ were markedly reduced, resulting in a net negative transport of pollutants, indicating that BJ was a source of pollutants for its environs. Combined with the results from Fig. 8c, there was net pollutant output to BJ's east and south. By analysing Fig. 8c and d, it can be seen that changes in the net transport rate for BJ correlated with the transport rate southward. This was principally because westerly input and easterly output were basically equal and so offset one another. The northward transport rate was consistently low, and the variable southward transport rate therefore had an enormous influence on the BJ area. These results indicate that pollutant transport between

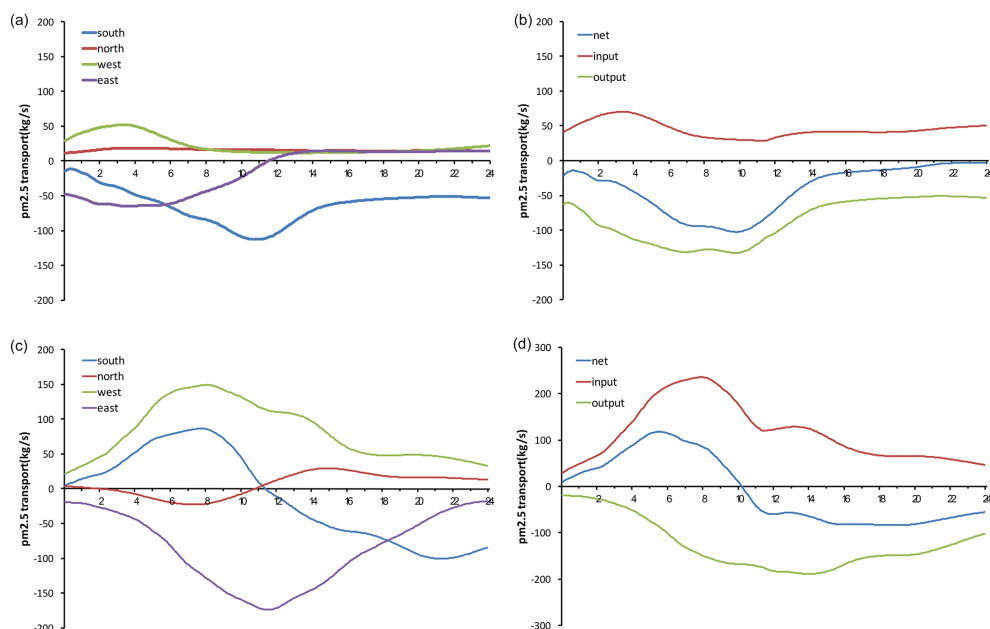


Figure 8. PM_{2.5} transport rates (kg s^{-1}) from S, N, W and E of BJ on (a) 6 and (c) 7 December. Total input, output and net PM_{2.5} transport rate (kg s^{-1}) from BJ's environs on (b) 6 and (d) 7 December.

BJ and its southern environs had the most significant impact on pollution levels in BJ in comparison to other areas.

4.4 Contribution of pollutant transport to PM_{2.5} concentrations over BJ

The observation studies of haze events in eastern China (Wang et al., 2014a) showed that “there is an aerosol extinction layer from the height of 1–1.5 km to 2–3 km from the ground, indicating most of the PM₁₀ pollutants are mainly concentrated in the near ground atmosphere layer below 1 km and a small part of pollutants can also spread to the height of more than 2–3 km from the ground”. In order to evaluate the contribution made by pollutants transported from its environs to BJ PM_{2.5} pollution, the total PM_{2.5} suspended in the atmosphere between the surface and a height of 3000 m over the BJ area during this haze episode was calculated, according to the formula

$$\text{Total}_{\text{PM}_{2.5}}(t) = \sum_{z=1}^7 \sum_{x=x_1}^{x_1} \sum_{y=y_1}^{y_2} \text{PM}(x, y, z, t) \cdot \Delta x(y, t) \cdot \Delta y(y, t) \cdot \Delta z(x, y, z, t),$$

along with the net hourly transport amount (Fig. 9). Total PM_{2.5} changed little during 6 December, but did rise slightly after a small decline at 12:00 UTC (20:00 LT), when the net hourly output transport value decreased. The total PM_{2.5} amount continued rising on 7 December and began to accelerate sharply until 09:00 UTC (17:00 LT) (4555.4 t), with a large net hourly input. After 12:00 UTC (20:00 LT), net hourly transport became highly negative, and total PM_{2.5} de-

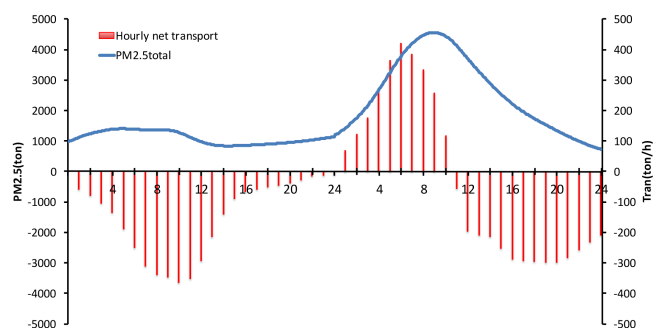
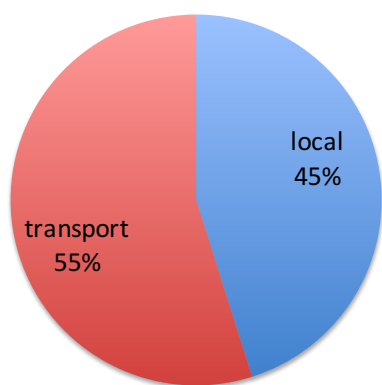
creased rapidly. By the end of 7 December, the total PM_{2.5} suspended in the atmosphere over BJ was consistent with the values for 6 December. As Fig. 9 shows, this sharp rise in total PM_{2.5} began at 12:00 UTC (20:00 LT) on 6 December (980 t), and ended at 12:00 UTC (20:00 LT) on 7 December (3707 t), when total PM_{2.5} reached its maximum value before beginning to decrease, and the total PM_{2.5} suspended over the BJ area increased by about 2727 t in this period. As the calculation results in Table 1 show, net input was 1497 t, accounting for 55 % of the total PM_{2.5} increase (2727 t) from 12:00 UTC (20:00 LT), 6 December, to 12:00 UTC (20:00 LT), 7 December. The remaining 1230 t could be attributed to local effects, and accounted for 45 % of the total PM_{2.5} increase (Fig. 10). This suggests that the transport of particle pollutants from its environs made a significant contribution to the peak PM_{2.5} values over BJ during this haze episode.

5 Conclusions

The GRAPES-CUACE online mesoscale chemical weather forecasting model was used to study the influence of PM transported from its near environs on high PM_{2.5} pollution levels in BJ during a severe haze episode on 6–7 December 2013. Simulated results were compared with ground-level horizontal visibility, haze weather phenomena as observed by CMA, and surface PM_{2.5} concentrations observed by CNEMC, to evaluate the model's ability to accurately describe haze pollution in China. The 3D wind field over the Jing–Jin–Ji region and its relationship with PM_{2.5} variations

Table 1. Total input, total output and total net transport (all in tons) for the BJ area for each time period (UTC and LT) during 6–7 December 2013.

Time (UTC)	Time (LT)	Input	Output	Net
00:00–12:00 6 Dec	08:00, 6 Dec–20:00, 6 Dec	2032	–4854	–2822
12:00–24:00, 6 Dec	20:00, 6 Dec–08:00, 7 Dec	1850	–2617	–767
00:00–12:00, 7 Dec	08:00, 7 Dec–20:00, 7 Dec	6551	–4288	2264
12:00–24:00, 7 Dec	20:00, 7 Dec–08:00, 8 Dec	3523	–6653	–3130
00:00–24:00, 6 Dec	08:00, 6 Dec–08:00, 7 Dec	3882	–7471	–3588
00:00–24:00, 7 Dec	08:00, 7 Dec–08:00, 8 Dec	10 074	–10 940	–866
00:00, 6 Dec–24:00, 7 Dec	08:00, 6 Dec–08:00, 8 Dec	13 956	–18 411	–4455
12:00, 6 Dec–12:00, 7 Dec	20:00, 6 Dec–20:00, 7 Dec	8401	–6905	1497

**Figure 9.** Total PM_{2.5} (ton) suspended in the atmosphere from the surface to 3000 m over the BJ area and the net hourly PM_{2.5} input (ton h⁻¹) for BJ during 6–7 December 2013.**Figure 10.** Contribution made by net transport and local effects to PM_{2.5} increases in BJ, 6–7 December 2013.

in BJ, the input/output pollutant transport rates for BJ and its N, S, E and W environs, the total input, output and net pollutant transport amounts for BJ, and the total PM_{2.5} suspended in the atmosphere over BJ, were all calculated in relation to the possible contribution of PM_{2.5} transported from its environs to the high PM_{2.5} pollution levels in BJ during the aforementioned severe haze episode. The results can be summarized as follows.

Table 2. Station locations

Station	Lat.	Long.	Alt. (m)
Beijing (BJ)	39.90	116.47	31.3
Shijiazhuang (SJZ)	38.05	114.43	80.5
Baoding (BD)	38.51	115.30	17.2
Cangzhou (CZ)	38.18	116.52	9.6
Dezhou (DZ)	37.26	116.17	21.2
Handan (HD)	36.36	114.28	58.2
Hengshui (HS)	37.44	115.42	24.3
Xingtai (XT)	37.04	114.30	76.8
Zhengzhou (ZZ)	34.73	113.70	110.4
Nanjing (NJ)	32.05	118.77	8.9
Shanghai (SH)	31.23	121.48	4.5

1. The spatial and temporal comparison of the simulated results with observational data showed that the model is capable of accurately describing haze episodes in China, and especially in the Jing–Jin–Ji region. This then formed a sound foundation for the calculation of PM transported across cities in this region.
2. There was a very close positive correlation between the southerly wind speed over the area to the south of BJ and PM_{2.5} variations in BJ, suggesting the likely important contribution made by PM transport from BJ's southern environs to the city. At 08:00 UTC (16:00 LT) on 7 December, southwesterlies from the surface to 800 hPa were largely stable in BJ and its southern environs; the region north of BJ was affected by a gentle wind. Both the southerly wind speed in the area to the south of BJ, and PM_{2.5}, reached their maxima at about 900 hPa, suggesting that this height served as the major transport layer for pollutants from the south to BJ.
3. The BJ area was a net output source for its environs for most of the haze episode during 6–7 December, except for the period from 00:00 to 10:00 UTC (08:00 to 18:00 LT), 7 December, when the haze was at its most serious and was accompanied by the highest PM_{2.5} values. Input from the west was more or less offset by

transport eastward. The input rate from the south was much higher than the output rate to the north from 00:00 to 10:00 UTC (08:00 to 18:00 LT), 7 December, and there was thus a net input during this period, resulting in the most serious pollution levels and peak PM_{2.5} values for this haze episode. This shows that pollutant transport from the south was the major contributor to the peak PM_{2.5} pollution levels in the BJ area.

- Total PM_{2.5} suspended in the atmosphere from the surface to 3000 m over the BJ area changed very little during 6 December. Total PM_{2.5} began to rise slightly at 12:00 UTC (20:00 LT), 6 December, when the net hourly output transport rate decreased; then rose clearly at 00:00 UTC (08:00 LT), 7 December; and was followed by a rising trend that maintained until 09:00 UTC (17:00 LT), 7 December, accompanied by high net hourly input values. After 12:00 UTC (20:00 LT), the net hourly transport rate became significantly negative as total PM_{2.5} decreased rapidly. Total PM_{2.5} suspended over BJ increased by about 2727 t from 12:00 UTC (20:00 LT), 6 December, to 12:00 UTC (20:00 LT), 7 December. The total net input was 1497 t, accounting for 55 % of the total PM_{2.5} increase during this period. The remaining 1230 t could be attributed to local effects, and accounted for 45 % of the total PM_{2.5} increase. This suggests that PM transport from its environs significantly influenced the peak PM_{2.5} values over BJ during this episode.

Acknowledgements. This work was supported by the National Basic Research Program (973) (grant no. 2014CB441201), the National Natural Scientific Foundation of China (grant nos. 41275007 and 41130104), the Jiangsu Collaborative Innovation Center for Climate Change–CAMS key projects (grant no. 2013Z007), the Science and Technology Support Program of Jiangsu Province (grant no. BE2012771), and the Priority Academic Program Development of Jiangsu Higher Education Institutions (PAPD).

Edited by: S. Gong

References

- An, X. Q., Sun, Z. B., Lin, W. L., Jin, M., and Li, N.: Emission inventory evaluation using observations of regional atmospheric background stations of China, *J. Environ. Sci.*, 25, 537–546, 2013.
- Cao, G., Zhang, X., and Zheng, F.: Inventory of black carbon and organic carbon 446 emissions from China, *Atmos. Environ.*, 40, 6516–6527, 2006.
- Cao, G. L., An, X. Q., Zhou, C. H., Ren, Y. Q., and Tu, J.: Emission inventory of air pollutants in China, *Chin. Environ. Sci.*, 30, 900–906, 2010.
- Chan, C. K. and Yao, X.: Air pollution in mega cities in China, *Atmos. Environ.*, 42, 1–42, doi:10.1016/j.atmosenv.2007.09.003, 2008.
- Chen, D., Xue, J., Yang, X., Zhang, H., Shen, X., Hu, J., Wang, Y., Ji, L., and Chen, J.: New generation of multi-scale NWP system (GRAPES): general scientific design, *Chinese Sci. Bull.*, 53, 3433–3445, doi:10.1007/s11434-008-0494-z, 2008.
- Chen, Y., Liu, Q., Geng, F., Zhang, H., Cai, C., Xu, T., Ma, X., and Li, H.: Vertical distribution of optical and micro-physical properties of ambient aerosols during dry haze periods in Shanghai, *Atmos. Environ.*, 50, 50–59, doi:10.1016/j.atmosenv.2012.01.002, 2012.
- Cheng, Y., Engling, G., He, K.-B., Duan, F.-K., Ma, Y.-L., Du, Z.-Y., Liu, J.-M., Zheng, M., and Weber, R. J.: Biomass burning contribution to Beijing aerosol, *Atmos. Chem. Phys.*, 13, 7765–7781, doi:10.5194/acp-13-7765-2013, 2013.
- Cheng, Z., Wang, S., Fu, X., Watson, J. G., Jiang, J., Fu, Q., Chen, C., Xu, B., Yu, J., Chow, J. C., and Hao, J.: Impact of biomass burning on haze pollution in the Yangtze River delta, China: a case study in summer 2011, *Atmos. Chem. Phys.*, 14, 4573–4585, doi:10.5194/acp-14-4573-2014, 2014.
- China Statistical Yearbook: 2012, 2013, National Bureau of Statistics of China, China Statistics Press, Beijing, 2012, 2013.
- CMA: Specifications for the Surface Meteorological Observations, Meteorological Press, Beijing, China, 2003 (in Chinese).
- Du, H., Kong, L., Cheng, T., Chen, J., Du, J., Li, L., Xia, X., Leng, C., and Huang, G.: Insights into summertime haze pollution events over Shanghai based on online water-soluble ionic composition of aerosols, *Atmos. Environ.*, 45, 5131–5137, doi:10.1016/j.atmosenv.2011.06.027, 2011.
- Duan, J., Guo, S., Tan, J., Wang, S., and Chai, F.: Characteristics of atmospheric carbonyls during haze days in Beijing, China, *Atmos. Res.*, 114–115, 17–27, doi:10.1016/j.atmosres.2012.05.010, 2012.
- Fu, X., Wang, S. X., Cheng, Z., Xing, J., Zhao, B., Wang, J. D., and Hao, J. M.: Source, transport and impacts of a heavy dust event in the Yangtze River Delta, China, in 2011, *Atmos. Chem. Phys.*, 14, 1239–1254, doi:10.5194/acp-14-1239-2014, 2014.
- Gong, S. L., Zhang, X. Y., Zhao, T. L., Mckendry, I. G., Jaffe, D. A., and Lu, N. M.: Characterization of soil dust aerosol in China and its transport and distribution during 2001 ACE-Asia: 2. Model simulation and validation, *J. Geophys. Res.*, 108, 4262, doi:10.1029/2002jd002633, 2003.
- Gong, S. L. and Zhang, X. Y.: CUACE/Dust – an integrated system of observation and modeling systems for operational dust forecasting in Asia, *Atmos. Chem. Phys.*, 8, 2333–2340, doi:10.5194/acp-8-2333-2008, 2008.
- Gurjar, B. R., Jain, A., Sharma, A., Agarwal, A., Gupta, P., Nagpure, A. S., and Lelieveld, J.: Human health risks in megacities due to air pollution, *Atmos. Environ.*, 44, 4606–4613, doi:10.1016/j.atmosenv.2010.08.011, 2010.
- Huang, K., Zhuang, G., Lin, Y., Wang, Q., Fu, J. S., Fu, Q., Liu, T., and Deng, C.: How to improve the air quality over megacities in China: pollution characterization and source analysis in Shanghai before, during, and after the 2010 World Expo, *Atmos. Chem. Phys.*, 13, 5927–5942, doi:10.5194/acp-13-5927-2013, 2013.
- Ji, D., Li, L., Wang, Y., Zhang, J., Cheng, M., Sun, Y., Liu, Z., Wang, L., Tang, G., Hu, B., Chao, N., Wen, T., and Miao, H.: The heaviest particulate air-pollution episodes occurred in northern China

- in January, 2013: insights gained from observation, *Atmos. Environ.*, 92, 546–556, doi:10.1016/j.atmosenv.2014.04.048, 2014.
- Kan, H., Chen, R., and Tong, S.: Ambient air pollution, climate change, and population health in China, *Environ Int.*, 42, 10–19, doi:10.1016/j.envint.2011.03.003, 2012.
- Kanakidou, M., Mihalopoulos, N., Kindap, T., Im, U., Vrekoussis, M., Gerasopoulos, E., Dermizaki, E., Unal, A., Koçak, M., Markakis, K., Melas, D., Kouvarakis, G., Youssef, A. F., Richter, A., Hatzianastassiou, N., Hilboll, A., Ebojje, F., Wittrock, F., von Savigny, C., Burrows, J. P., Ladstaetter-Weissenmayer, A., and Moubasher, H.: Megacities as hot spots of air pollution in the East Mediterranean, *Atmos. Environ.*, 45, 1223–1235, doi:10.1016/j.atmosenv.2010.11.048, 2011.
- Kang, E., Han, J., Lee, M., Lee, G., and Kim, J. C.: Chemical characteristics of size-resolved aerosols from Asian dust and haze episode in Seoul Metropolitan City, *Atmos. Res.*, 127, 34–46, doi:10.1016/j.atmosres.2013.02.002, 2013.
- Kang, H., Zhu, B., Su, J., Wang, H., Zhang, Q., and Wang, F.: Analysis of a long-lasting haze episode in Nanjing, China, *Atmos. Res.*, 120–121, 78–87, doi:10.1016/j.atmosres.2012.08.004, 2013.
- Liu, Q., Liu, Y., Yin, J., Zhang, M., and Zhang, T.: Chemical characteristics and source apportionment of PM₁₀ during Asian dust storm and non-dust storm days in Beijing, *Atmos. Environ.*, 91, 85–94, doi:10.1016/j.atmosenv.2014.03.057, 2014.
- Liu, W.-T., Hsieh, H.-C., Chen, S.-P., Chang, J. S., Lin, N.-H., Chang, C.-C., and Wang, J.-L.: Diagnosis of air quality through observation and modeling of volatile organic compounds (VOCs) as pollution tracers, *Atmos. Environ.*, 55, 56–63, doi:10.1016/j.atmosenv.2012.03.017, 2012.
- Quan, J., Tie, X., Zhang, Q., Liu, Q., Li, X., Gao, Y., and Zhao, D.: Characteristics of heavy aerosol pollution during the 2012–2013 winter in Beijing, China, *Atmos. Environ.*, 88, 83–89, doi:10.1016/j.atmosenv.2014.01.058, 2014.
- Salinas, S. V., Chew, B. N., Miettinen, J., Campbell, J. R., Welton, E. J., Reid, J. S., Yu, L. E., and Liew, S. C.: Physical and optical characteristics of the October 2010 haze event over Singapore: a photometric and lidar analysis, *Atmos. Res.*, 122, 555–570, doi:10.1016/j.atmosres.2012.05.021, 2013.
- Tan, J., Guo, S., Ma, Y., Duan, J., Cheng, Y., He, K., and Yang, F.: Characteristics of particulate PAHs during a typical haze episode in Guangzhou, China, *Atmos. Res.*, 102, 91–98, doi:10.1016/j.atmosres.2011.06.012, 2011.
- Tan, J., Yang, L., Grimmond, C. S. B., Shi, J., Gu, W., Chang, Y., Hu, P., Sun, J., Ao, X., and Han, Z.: Urban Integrated Meteorological Observations: Practice and Experience in Shanghai, China, *Bull. Am. Meteorol. Soc.*, 96, 85–102, doi:10.1175/bams-d-13-00216.1, 2015.
- Wang, G., Chen, C., Li, J., Zhou, B., Xie, M., Hu, S., Kawamura, K., and Chen, Y.: Molecular composition and size distribution of sugars, sugar-alcohols and carboxylic acids in airborne particles during a severe urban haze event caused by wheat straw burning, *Atmos. Environ.*, 45, 2473–2479, doi:10.1016/j.atmosenv.2011.02.045, 2011.
- Wang, H., Gong, S., Zhang, H., Chen, Y., Shen, X., Chen, D., Xue, J., Shen, Y., Wu, X., and Jin, Z.: A new-generation sand and dust storm forecasting system GRAPES_CUACE/Dust: model development, verification and numerical simulation, *Chinese Sci. Bull.*, 55, 635–649, doi:10.1007/s11434-009-0481-z, 2009.
- Wang, H., Zhang, X. Y., Gong, S. L., Chen, Y., Shi, G. Y., and Li, W.: Radiative feedback of dust aerosols on the East Asian dust storms, *J. Geophys. Res.*, 115, D23214, doi:10.1029/2009jd013430, 2010.
- Wang, H., Shi, G., Zhu, J., Chen, B., Che, H., and Zhao, T.: Case study of longwave contribution to dust radiative effects over East Asia, *Chinese Sci. Bull.*, 58, 3673–3681, doi:10.1007/s11434-013-5752-z, 2013.
- Wang, H., Tan, S.-C., Wang, Y., Jiang, C., Shi, G.-Y., Zhang, M.-X., and Che, H.-Z.: A multisource observation study of the severe prolonged regional haze episode over eastern China in January 2013, *Atmos. Environ.*, 89, 807–815, doi:10.1016/j.atmosenv.2014.03.004, 2014a.
- Wang, H., Xu, J., Zhang, M., Yang, Y., Shen, X., Wang, Y., Chen, D., and Guo, J.: A study of the meteorological causes of a prolonged and severe haze episode in January 2013 over central-eastern China, *Atmos. Environ.*, 98, 146–157, doi:10.1016/j.atmosenv.2014.08.053, 2014b.
- Wang, H., Shi, G. Y., Zhang, X. Y., Gong, S. L., Tan, S. C., Chen, B., Che, H. Z., and Li, T.: Mesoscale modelling study of the interactions between aerosols and PBL meteorology during a haze episode in China Jing–Jin–Ji and its near surrounding region – Part 2: Aerosols’ radiative feedback effects, *Atmos. Chem. Phys.*, 15, 3277–3287, doi:10.5194/acp-15-3277-2015, 2015a.
- Wang, H., Xue, M., Zhang, X. Y., Liu, H. L., Zhou, C. H., Tan, S. C., Che, H. Z., Chen, B., and Li, T.: Mesoscale modeling study of the interactions between aerosols and PBL meteorology during a haze episode in Jing–Jin–Ji (China) and its nearby surrounding region – Part 1: Aerosol distributions and meteorological features, *Atmos. Chem. Phys.*, 15, 3257–3275, doi:10.5194/acp-15-3257-2015, 2015b.
- Wang, L., Xu, J., Yang, J., Zhao, X., Wei, W., Cheng, D., Pan, X., and Su, J.: Understanding haze pollution over the southern Hebei area of China using the CMAQ model, *Atmos. Environ.*, 56, 69–79, doi:10.1016/j.atmosenv.2012.04.013, 2012.
- Wang, L. T., Wei, Z., Yang, J., Zhang, Y., Zhang, F. F., Su, J., Meng, C. C., and Zhang, Q.: The 2013 severe haze over southern Hebei, China: model evaluation, source apportionment, and policy implications, *Atmos. Chem. Phys.*, 14, 3151–3173, doi:10.5194/acp-14-3151-2014, 2014.
- Wu, D., Tie, X., Li, C., Ying, Z., Kai-Hon Lau, A., Huang, J., Deng, X., and Bi, X.: An extremely low visibility event over the Guangzhou region: a case study, *Atmos. Environ.*, 39, 6568–6577, doi:10.1016/j.atmosenv.2005.07.061, 2005.
- Wu, D., Wu, X. J., Li, F., Tan, H. B., Chen, J., Cao, Z. Q., Sun, X., Chen, H. H., and Li, H. Y.: Temporal and spatial variation of haze during 1951–2005 in Chinese mainland. *Meteorologica Sinica*, 68, 680–688, doi:10.11676/qxxb2010.066, 2010.
- Xu, G., Chen, D., Xue, J., Sun, J., Shen, X., Shen, Y., Huang, L., Wu, X., Zhang, H., and Wang, S.: The program structure designing and optimizing tests of GRAPES physics, *Chinese Sci. Bull.*, 53, 3470–3476, doi:10.1007/s11434-008-0418-y, 2008.
- Xu, H. M., Tao, J., Ho, S. S. H., Ho, K. F., Cao, J. J., Li, N., Chow, J. C., Wang, G. H., Han, Y. M., Zhang, R. J., Watson, J. G., and Zhang, J. Q.: Characteristics of fine particulate non-polar organic compounds in Guangzhou during the 16th Asian Games: effectiveness of air pollution controls, *Atmos. Environ.*, 76, 94–101, doi:10.1016/j.atmosenv.2012.12.037, 2013.

- Xue, J., Zhuang, S., Zhu, G., Zhang, H., Liu, Z., Liu, Y., and Zhuang, Z.: Scientific design and preliminary results of three-dimensional variational data assimilation system of GRAPES, *Chinese Sci. Bull.*, 53, 3446–3457, doi:10.1007/s11434-008-0416-0, 2008.
- Yang, X., Hu, J., Chen, D., Zhang, H., Shen, X., Chen, J., and Ji, L.: Verification of GRAPES unified global and regional numerical weather prediction model dynamic core, *Chinese Sci. Bull.*, 53, 3458–3464, doi:10.1007/s11434-008-0417-z, 2008.
- Ying, Q., Wu, L., and Zhang, H.: Local and inter-regional contributions to PM_{2.5} nitrate and sulfate in China, *Atmos. Environ.*, 94, 582–592, doi:10.1016/j.atmosenv.2014.05.078, 2014.
- Yu, X., Zhu, B., Yin, Y., Yang, J., Li, Y., and Bu, X.: A comparative analysis of aerosol properties in dust and haze-fog days in a Chinese urban region, *Atmos. Res.*, 99, 241–247, doi:10.1016/j.atmosres.2010.10.015, 2011.
- Zhang, R. and Shen, X.: On the development of the GRAPES – a new generation of the national operational NWP system in China, *Chinese Sci. Bull.*, 53, 3429–3432, doi:10.1007/s11434-008-0462-7, 2008.
- Zhang, S., Wu, Y., Wu, X., Li, M., Ge, Y., Liang, B., Xu, Y., Zhou, Y., Liu, H., Fu, L., and Hao, J.: Historic and future trends of vehicle emissions in Beijing, 1998–2020: A policy assessment for the most stringent vehicle emission control program in China, *Atmos. Environ.*, 89, 216–229, doi:10.1016/j.atmosenv.2013.12.002, 2014.
- Zhang, X. Y., Gong, S. L., Zhao, T. L., Arimoto, R., Wang, Y. Q., and Zhou, Z. J.: Sources of Asian dust and role of climate change versus desertification in Asian dust emission, *Geophys. Res. Lett.*, 30, 2272, doi:10.1029/2003gl018206, 2003.
- Zhou, C. H., Gong, S. L., Zhang, X. Y., Wang, Y. Q., Niu, T., Liu, H. L., Zhao, T. L., Yang, Y. Q., and Hou, Q.: Development and evaluation of an operational SDS forecasting system for East Asia: CUACE/Dust, *Atmos. Chem. Phys.*, 8, 787–798, doi:10.5194/acp-8-787-2008, 2008.
- Zhu, G., Xue, J., Zhang, H., Liu, Z., Zhuang, S., Huang, L., and Dong, P.: Direct assimilation of satellite radiance data in GRAPES variational assimilation system, *Chinese Sci. Bull.*, 53, 3465–3469, doi:10.1007/s11434-008-0419-x, 2008.